Electronic Supplementary Information (ESI) for Chemical Communications
This journal is (c) The Royal Society of Chemistry 2013

Electronic Supplementary Information

Fe–Co bimetallic alloy nanoparticles as a highly active peroxidase mimetic and its application in biosensing

Yujin Chen,[a] Haiyan Cao,[a] Wenbing Shi,[c] Hong Liu,*[b] Yuming Huang*[a]

[a] *State Key Laboratory Breeding Base of Eco-Environments and Bio-Resources of the Three Gorges Reservoir Region; College of Chemistry and Chemical Engineering, Southwest University, Chongqing 400715, PR China*

[b] *Chongqing Institute of Green and Intelligent Technology, Chongqing 401122, P.R. China*

[c] *College of Chemistry and Chemical Engineering, Yangtze Normal University Fuling, Chongqing 408003, P. R. China*

Materials and methods

Chemicals and reagents

Sodium borohydride was from Aladdin (Aladdin Chemistry Co, Ltd, 98%). Polyvinylpyrrolidone K30 (PVP, $(C_6H_9NO)_n$), glucose, fructose, lactose, and maltose were purchased from Sinopharm Chemical Reagent Co. Ltd (Shanghai, China). 3,3,5,5-tetramethylbenzidine (TMB) and glucose oxidase (GOx) were purchased from Sigma-Aldrich and stored in a refrigerator at 4 °C. Iron(II) chloride tetrahydrate ($FeCl_2$•$4H_2O$, >99%), cobaltous(II) chloride hexahydrate ($CoCl_2$•$6H_2O$, >99%), H_2O_2, acetic acid, sodium acetate, and ethanol were obtained from Chongqing Chemical Reagents Company (Chongqing, China). All other chemicals were of analytical reagent grade and used without further purification. All solutions were prepared using ultra pure water.

Instrumentation

Absorption measurements were performed on a UV-2450 spectrophotometer (Shimadzu, Japan). The pH of the solution was detected by a PHS-3D precision pH meter (Shanghai Precision Scientific Instruments Co., Ltd., China). Transmission electron microscopy (TEM) images were captured on a FEI Tecnai G20 ST equipped with an energy dispersive X-ray spectrometer (EDX) for elemental analysis. An XSAM800 X-ray photoelectron spectrometer (Kratos, Britain) was used to the surface analysis of the as-prepared material. The X-ray diffraction (XRD) patterns of the as-prepared material were measured using an XD-3 X-ray diffractometer (PuXi, Beijing, China) under the conditions of nickel filtered Cu-Ka radiation (λ=0.15406 nm) at current of 20 mA and a voltage of 36 kV. The scanning rate was 4 deg min^{-1} in the angular range of 10–70º (2θ).

Synthesis of $Fe_{1-x}Co_x$ NPs (x = 0, 0.3, 0.4, 0.5, 0.6, 0.7 and 1)

$Fe_{1-x}Co_x$ NPs with different molar ratios were obtained by varying the initial concentration of Fe and Co salts in solution. The molar ratio of metal salts (namely, $FeCl_2$+$CoCl_2$) to $NaBH_4$ was kept at constant of 1:5. $Fe_{1-x}Co_x$ NPs were prepared as follows: $FeCl_2$•$4H_2O$ and $CoCl_2$·$6H_2O$ were dissolved with PVP (300 mg) in 30 mL

of distilled water, then $NaBH_4$ (264.8 mg) was added to the mixture rapidly with vigorous stirring under ambient condition. The original color of the metal precursor solutions (green for iron (II) chloride and purple for cobalt(II) chloride) was quickly change to grey or black, indicating that the $Fe_{1-x}Co_x$ (x = 0, 0.3, 0.4, 0.5, 0.6, 0.7 and 1) alloy NPs were formed. When no more hydrogen evolution was observed, the reaction was completed. The as-prepared $Fe_{1-x}Co_x$ NPs (x = 0, 0.3, 0.4, 0.5, 0.6, 0.7 and 1) were washed three times with distilled water and ethanol and dried in vacuum at 60 °C for 4 h. The as-prepared $Fe_{1-x}Co_x$ NPs (x = 0, 0.3, 0.4, 0.5, 0.6, 0.7 and 1) were stored in a desiccator for characterization. The stock solution of the as-prepared $Fe_{1-x}Co_x$ NPs was obtained by adding proper amount of dry $Fe_{1-x}Co_x$ NPs to ethanol.

Electron spin resonance

175 μL samples were prepared at room temperature by adding 5 μL of 3% H_2O_2, and 20 μL of 0.2 M DMPO (5,5-dimethyl-1-pyrroline *N*-oxide) and proper amount of 0.2 M NaAc buffer (pH 3.5) into a 1 mL plastic tube in the presence and absence of 50 μL of the as-prepared NPs ($Fe_{0.5}Co_{0.5}$ NPs, Fe NPs or Co NPs) with and without 5 μL of 0.01 M TMB, respectively. The prepared sample solution was transferred to a quartz capillary tube and placed in the ESR cavity. DMPO was used to trap the ·OH radicals to form the DMPO/·OH spin adduct. The ESR spectra were obtained on a Bruker ESR 300E with microwave bridge (receiver gain, 1×10^5; modulation amplitude, 2 Gauss; microwave power, 10 mW; modulation frequency, 100 kHz).

Kinetic analysis

Kinetic measurements were carried out in time course mode by monitoring the absorbance change at 652 nm. To investigate the mechanism, assays were carried out by varying concentrations of TMB at a fixed concentration of H_2O_2 or vice versa. With $Fe_{0.5}Co_{0.5}$ NPs as the catalyst, the reaction was carried out at 35 °C with 3.5 μg mL^{-1} $Fe_{0.5}Co_{0.5}$ NPs in 2.43 mL reaction buffer (0.2 mol L^{-1} NaAc, pH 4.0) in the presence of varied concentrations of TMB. With Fe NPs or Co NPs as the catalyst, the reaction was carried out at 45 °C with 3.5 μg mL^{-1} Fe NPs or

Co NPs in 2.43 mL of 0.1 mol L^{-1} reaction buffer (0.2 mol L^{-1} NaAc, pH = 3.5) in the presence of varied concentrations of TMB. The Michaelis-Menten behavior of the as-prepared NPs was studied. The apparent steady-state kinetic measurements were carried out under the experimental conditions as described above by varying concentration of TMB at a fixed concentration of H_2O_2 or vice versa unless otherwise stated. The apparent kinetic parameters were calculated based on the function $v = V_{max}\times[S]/(K_m+[S])$, where v is the initial velocity, V_{max} is the maximal reaction velocity, [S] is the concentration of substrate (H_2O_2), K_m is the Michaelis constant and K_m approximates the affinity of the enzyme for the substrate. The K_m and V_{max} were obtained from Lineweaver–Burk plots (Table S2 ESI†). The K_m value of the $Fe_{0.5}Co_{0.5}$ NPs for H_2O_2 was 0.06 mM, which is obviously lower than Fe NPs and Co NPs, and at least one order of magnitude lower than that of the HRP and other NPs-based peroxidase mimetic. It suggested that it had a much higher affinity to H_2O_2 than HRP and other mimics. On the other hand, the K_m value of the $Fe_{0.5}Co_{0.5}$ NPs for TMB was 1.79 mM, which was slightly higher than that of HRP, consistent with the results that a higher concentration of TMB was required to obtain maximal reaction velocity for $Fe_{0.5}Co_{0.5}$ NPs. The double–reciprocal plots (Fig. S9c,d ESI†) revealed the characteristic parallel lines of a ping-pong mechanism and implied that, like HRP, the Fe–Co bimetallic NPs bind and react with the first substrate, then release the first product before reacting with the second substrate.

General procedure for colorimetric detection and glucose analysis

In a typical process, the solution of hydrogen peroxide with a given concentration was added to TMB (final concentration of 5×10^{-5} M) solution in the presence of the $Fe_{0.5}Co_{0.5}$ NPs solution (final concentration of 3.5 mg L^{-1}) and the NaAc buffer (pH 4.0). The mixture was incubated at 35 °C for 20 min. Then UV-Vis spectra measurements and photographs were taken.

For glucose detection, the calibration curve for glucose was realized as follows: a) 0.1 mL of 1 mg mL^{-1} GOx was added to 0.1 mL of glucose with different concentrations in 0.5 mL of 10 mM NaAc buffer (pH 7.0) and the mixture was incubated at 37 °C for 30 min (with final glucose concentration of 0.5–10 μM); b) the resulting solution was mixed with 0.25 mL of 1 mM TMB, 0.1 mL of $Fe_{0.5}Co_{0.5}$ NPs (175 mg L^{-1}), and 3.95 mL of 0.2 M NaAc buffer (pH 4.0) for another 20 min of incubation at 35 °C; c) the obtained solution was used for standard curve measurement.

For glucose determination in serum, the serum samples from local hospital were first treated by ultra filtration with 3 kDa Amicon cell at 3000 rpm for 30 min. After 40-fold dilution of the obtained filtrate, 0.1 mL of the diluted filtrate was added into 0.5 mL of 10 mM NaAc buffer (pH 7.0) and 0.1 mL of 1 mg mL^{-1} GOx. After the obtained mixed solution was incubated at 37 °C for 30 min, the resulting solution was mixed with 0.25 mL of 1 mM TMB, 0.1 mL of $Fe_{0.5}Co_{0.5}$ NPs (175 mg L^{-1}), and 3.95 mL of 0.2 M NaAc buffer (pH 4.0) for another 20 min of incubation at 35 °C. Finally, the obtained solution was used for glucose determination. The results were compared with those by the conventional method. The comparison study was carried out by an OneTouch Ultra glucose meter (Johnson and Johnson Medical Ltd., Shanghai, China).

Table S1. Reproducibility between different batches of the as-prepared Fe–Co alloy NPs using the same preparation method.

Batch No.	1	2	3	RSD (%)
Catalytic activity (%)	100±6.1 [a]	92.1±4.6 [a]	96.8±2.1 [a]	4.0

[a] RSD for three duplicate determinations.

Table S2. Comparison of the apparent Michaelis–Menten constant (K_m) and maximal velocity (V_{max}) of the $Fe_{0.5}Co_{0.5}$ NPs and other NPs-based peroxidase mimetics and horseradish peroxidase (HRP)

	K_m/mmol L^{-1}		V_{max}/mol L^{-1} s^{-1}		
Catalyst	**H_2O_2**	**TMB**	**H_2O_2**	**TMB**	**Reference**
$Fe_{0.5}Co_{0.5}$ NPs	0.06	1.79	1.32×10^{-7}	4.56×10^{-7}	This work
Fe NPs	0.32	0.38	4.10×10^{-7}	2.38×10^{-7}	This work
Co NPs	1.14	5.09	1.72×10^{-8}	9.98×10^{-8}	This work
HRP	3.70	0.434	0.871×10^{-7}	1.00×10^{-7}	1
Fe_3O_4 MNPs	154	0.098	9.78×10^{-8}	3.44×10^{-8}	1
BSA-Au	25.3	0.00253	7.21×10^{-8}	6.23×10^{-8}	2
Pt-Ft	187.25	0.22	0.32	5.58×10^{-4}	3
$Au@Pt_{0.17}$	/	0.0095	/	10.2×10^{-8}	4
Co_3O_4	140.07	0.037	1.21×10^{-7}	6.27×10^{-8}	5
CGN	245	0.12	2.85×10^{-7}	3.32×10^{-7}	6
CuO	41	0.016	/	/	7
C-Dots	26.77	0.039	3.06×10^{-7}	3.61×10^{-8}	8
GO-COOH	3.99	0.0237	3.85×10^{-8}	3.45×10^{-8}	9
H-GNs	2.256	5.100	5.06×10^{-8}	4.55×10^{-8}	10
FeS	7.2	0.13	/	/	11
DIONrods	1.3	0.5	9.8×10^{-8}	11.6×10^{-8}	12
PBMNPs	323.6	0.307	1.17×10^{-6}	1.06×10^{-6}	13
$ZnFe_2O_4$ MNPs	1.66	0.85	7.74×10^{-8}	1.33×10^{-7}	14

References

[1] L. Gao, J. Zhuang, L. Nie, J. Zhang, Y. Zhang, N. Gu, T. Wang, J. Feng, D. Yang, S. Perrett, X. Yan, *Nat Nanotechnol*, 2007, **2,** 577–583.
[2] X.-X. Wang, Q. Wu, Z. Shan, Q.-M. Huang, *Biosens Bioelectron*, 2011, **26**, 3614–3619.
[3] J. Fan, J.-J. Yin, B. Ning, X. Wu, Y. Hu, M. Ferrari, G.J. Anderson, J. Wei, Y. Zhao, G. Nie, *Biomaterials*, 2011, **32** 1611–1618.
[4] W. He, Y. Liu, J. Yuan, J.-J. Yin, X. Wu, X. Hu, K. Zhang, J. Liu, C. Chen, Y. Ji, Y. Guo, *Biomaterials*, 2011, **32**,1139–1147.
[5] J. Mu, Y. Wang, M. Zhao, L. Zhang, *Chem Commun*, 2012, **48**, 2540–2542.
[6] J. Yin, H. Cao, Y. Lu, *J Mater Chem*, 2012, **22**, 527–534.
[7] W. Chen, J. Chen, Y.-B. Feng, L. Hong, Q.-Y. Chen, L.-F. Wu, X.-H. Lin, X.-H. Xia, *Analyst*, 2012, **137,** 1706–1712.
[8] W. Shi, Q. Wang, Y. Long, Z. Cheng, S. Chen, H. Zheng, Y. Huang, *Chem Commun*, 2011, **47,** 6695–6697.
[9] Y. Song, K. Qu, C. Zhao, J. Ren, X. Qu, *Adv Mater*, 2010, **22,** 2206–2210.
[10] Y. Guo, L. Deng, J. Li, S. Guo, E. Wang, S. Dong, *ACS Nano*, 2011, **5,** 1282–1290.
[11] Z. Dai, S. Liu, J. Bao, H. Ju, *Chem–Eur J*, 2009, **15,** 4321–4326.
[12] S. Nath, C. Kaittanis, V. Ramachandran, N.S. Dalal, J.M. Perez, *Chem Mater*, 2009, **21,** 1761–1767.
[13] X.-Q. Zhang, S.-W. Gong, Y. Zhang, T. Yang, C.-Y. Wang, N. Gu, *J Mater Chem*, 2010, **20,** 5110–5116.
[14] L. Su, J. Feng, X. Zhou, C. Ren, H. Li, X. Chen, *Anal Chem*, 2012, **84,** 5753–5758.

Table S3. Results of determination of glucose in serum samples.

Serum	Proposed method (mM, n=3) [a]	Glucose meter method (mM) [b]
1	4.04 ± 0.10	4.8
2	6.74 ± 0.39	6.3
3	7.98 ± 0.79	7.8

[a] The blood samples were diluted 2000-fold for glucose determination by the proposed method.

[b] The glucose determination was performed directly without dilution in the laboratory for clinical analysis, The Ninth People's Hospital of Chongqing.

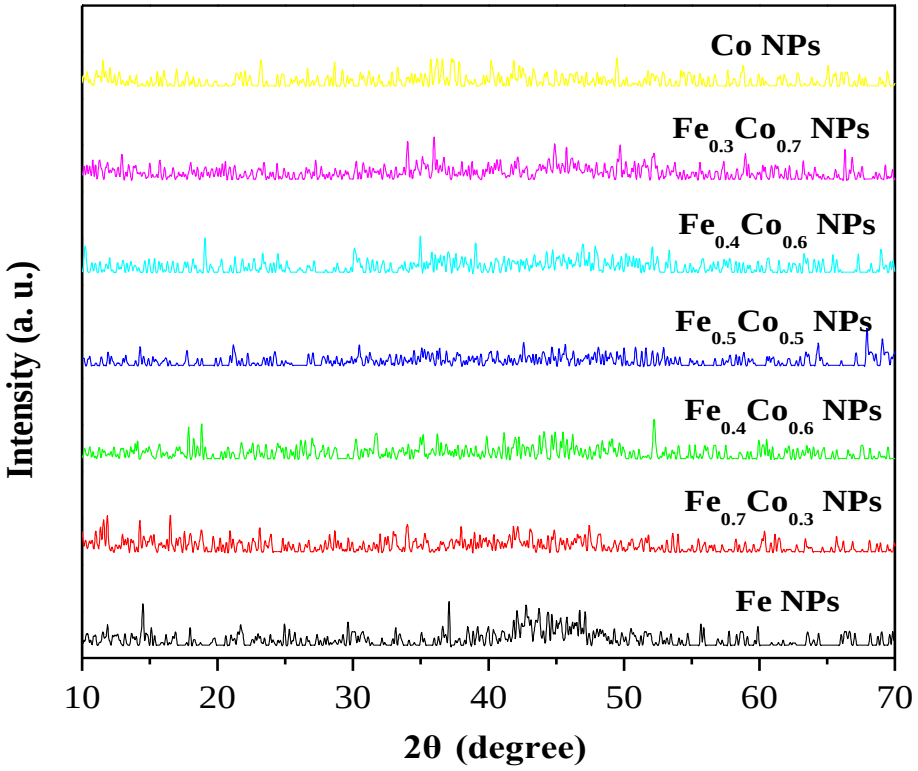

Figure S1. XRD patterns of the $Fe_{1-x}Co_x$ (x = 0, 0.3, 0.4, 0.5, 0.6, 0.7 and 1) NPs.

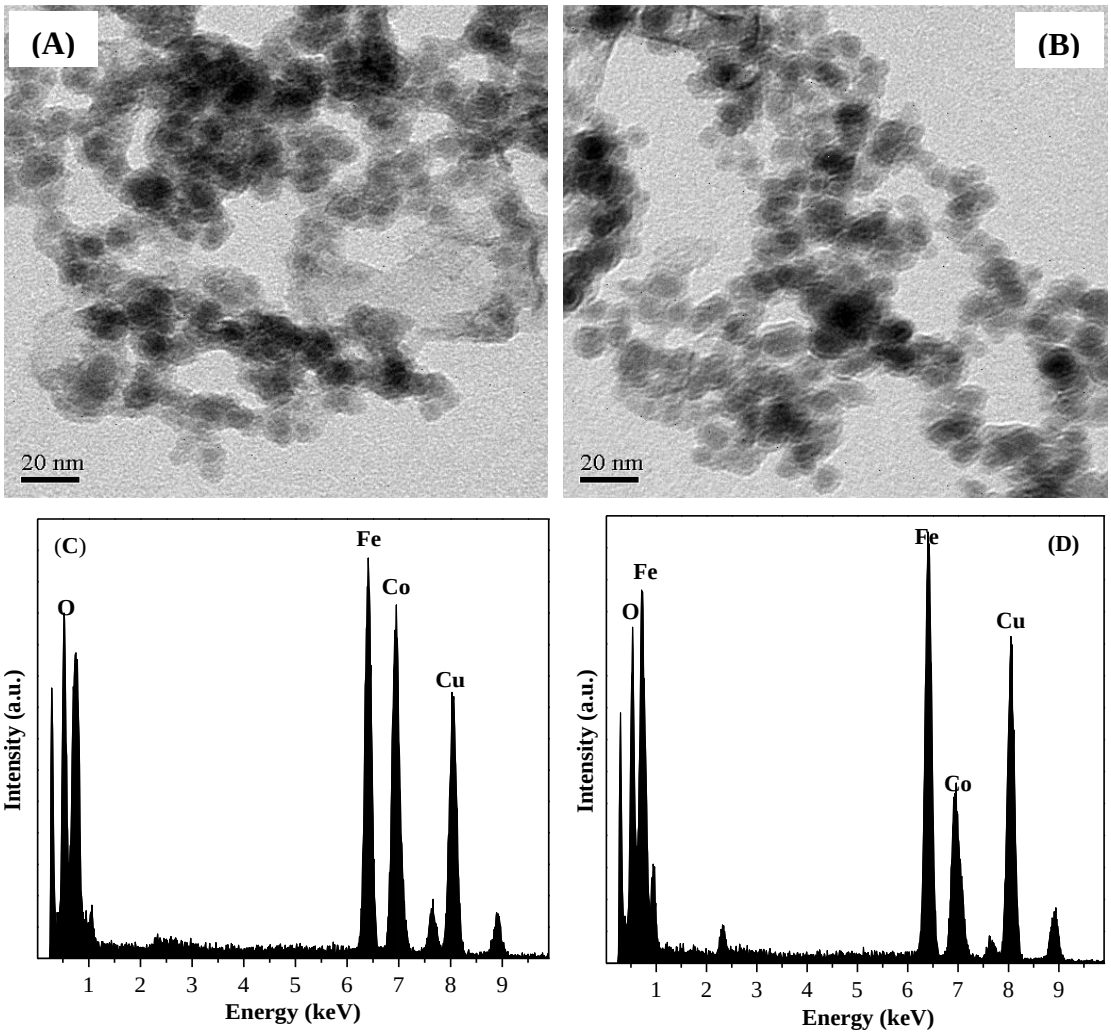

Figure S2. TEM images of $Fe_{0.5}Co_{0.5}$ alloy NPs (A) and $Fe_{0.7}Co_{0.3}$ alloy NPs (B). EDX spectra of $Fe_{0.5}Co_{0.5}$ alloy NPs (C) and $Fe_{0.7}Co_{0.3}$ alloy NPs (D).

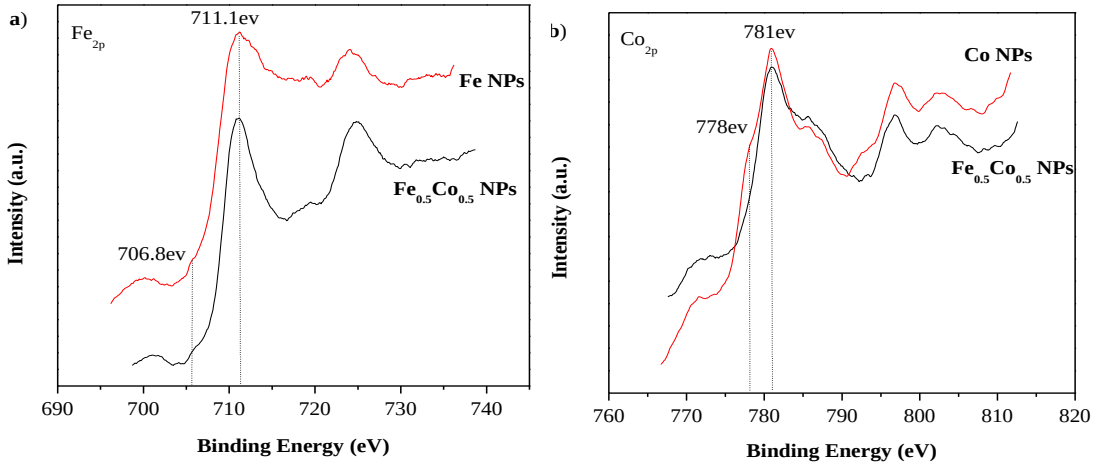

Figure S3. XPS spectra of Fe 2p (a) and Co 2p (b) level for Fe NPs, $Fe_{0.5}Co_{0.5}$ NPs and Co NPs.

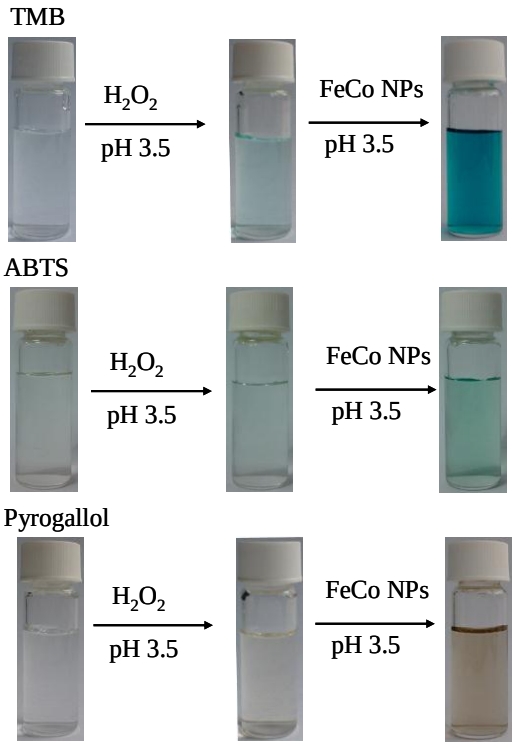

Figure S4. Images of oxidation color reaction of TMB, ABTS, and pyrogallol by H_2O_2 after catalyzing by Fe–Co alloy NPs at pH 3.5 NaAc buffer solution.

Supplementary Material (ESI) for Chemical Communications
This journal is (c) The Royal Society of Chemistry 2013

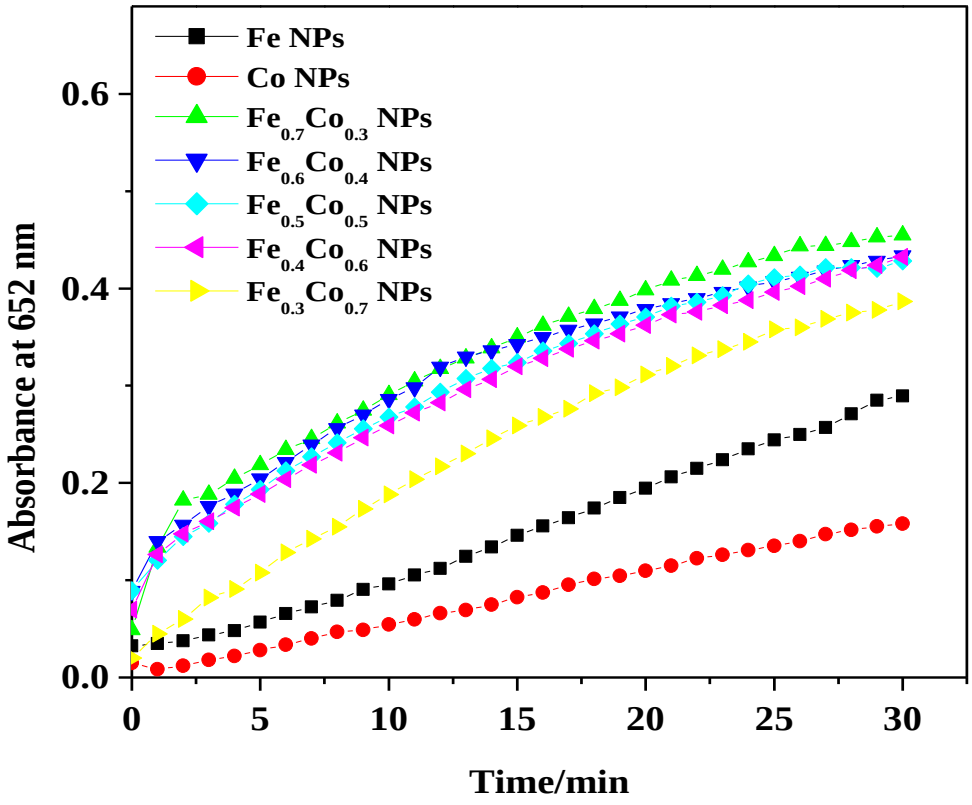

Figure S5. Composition dependence of catalytic activity of the Fe–Co alloy NPs. Conditions: 1 mM H_2O_2, 3.5 μg mL^{-1} catalyst, 50 μM TMB, pH 4.0 acetate buffers at 35 °C.

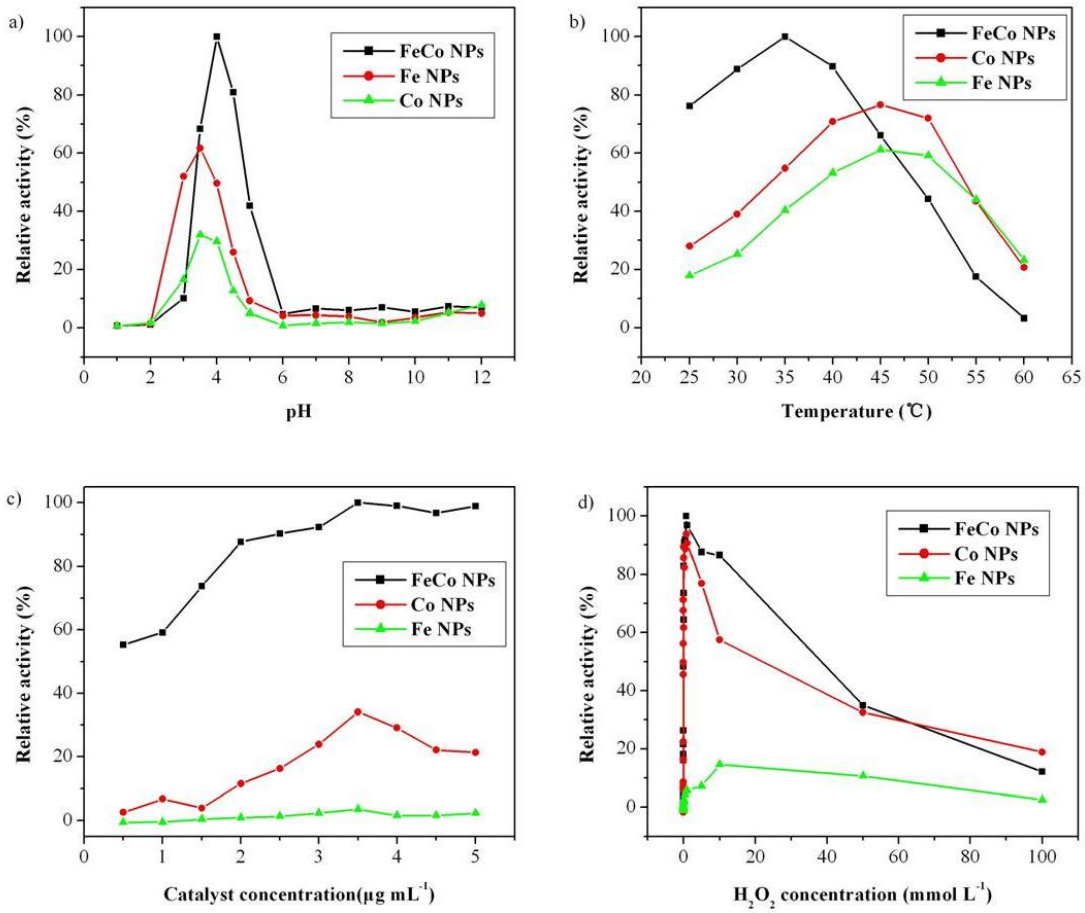

Figure S6. a) Effect of pH. Conditions: 3.5 μg mL^{-1} catalyst, 50 μM TMB, 35 °C, 1 mM H_2O_2. b) Effect of temperature. Conditions: 3.5 μg mL^{-1} catalyst, 50 μM TMB, 1 mM H_2O_2, pH 4.0 acetate buffers for $Fe_{0.5}Co_{0.5}$ NPs, pH 3.5 acetate buffers for Fe NPs and Co NPs. c) Effect of catalyst concentration. Conditions: 50 μM TMB, 1 mM H_2O_2, pH 4.0 acetate buffers at 35 °C for $Fe_{0.5}Co_{0.5}$ NPs, pH 3.5 acetate buffers at 45°C for Fe NPs and Co NPs. d) Effect of H_2O_2 concentration. Conditions: 3.5 μg mL^{-1} catalyst, 50 μM TMB, pH 4.0 acetate buffers at 35 °C for $Fe_{0.5}Co_{0.5}$ NPs, pH 3.5 acetate buffers at 45°C for Fe NPs and Co NPs.

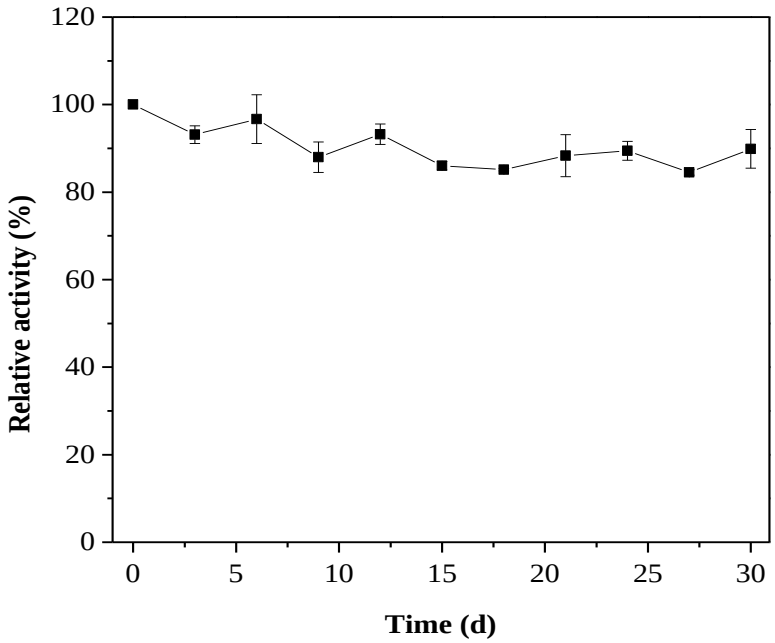

Figure S7. Variation of catalytic activity of the Fe–Co NPs with time.

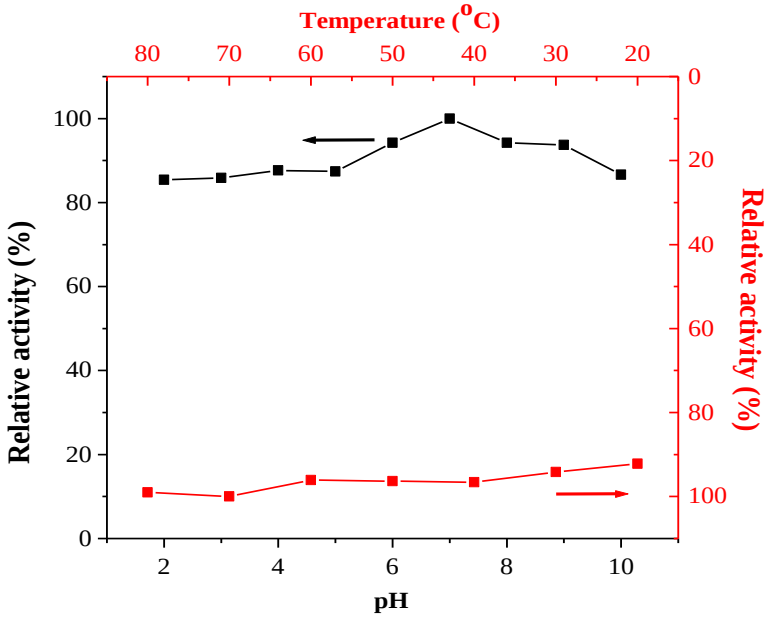

Figure S8. The stability of the Fe–Co NPs. Fe–Co NPs were first incubated at pH 2.0–10.0 for 2 h and then the peroxidase activity was measured under standard conditions (black line). Fe–Co NPs were first incubated at 20–80 °C for 2 h and then the peroxidase activity was measured under standard conditions (red line).

Supplementary Material (ESI) for Chemical Communications
This journal is (c) The Royal Society of Chemistry 2013

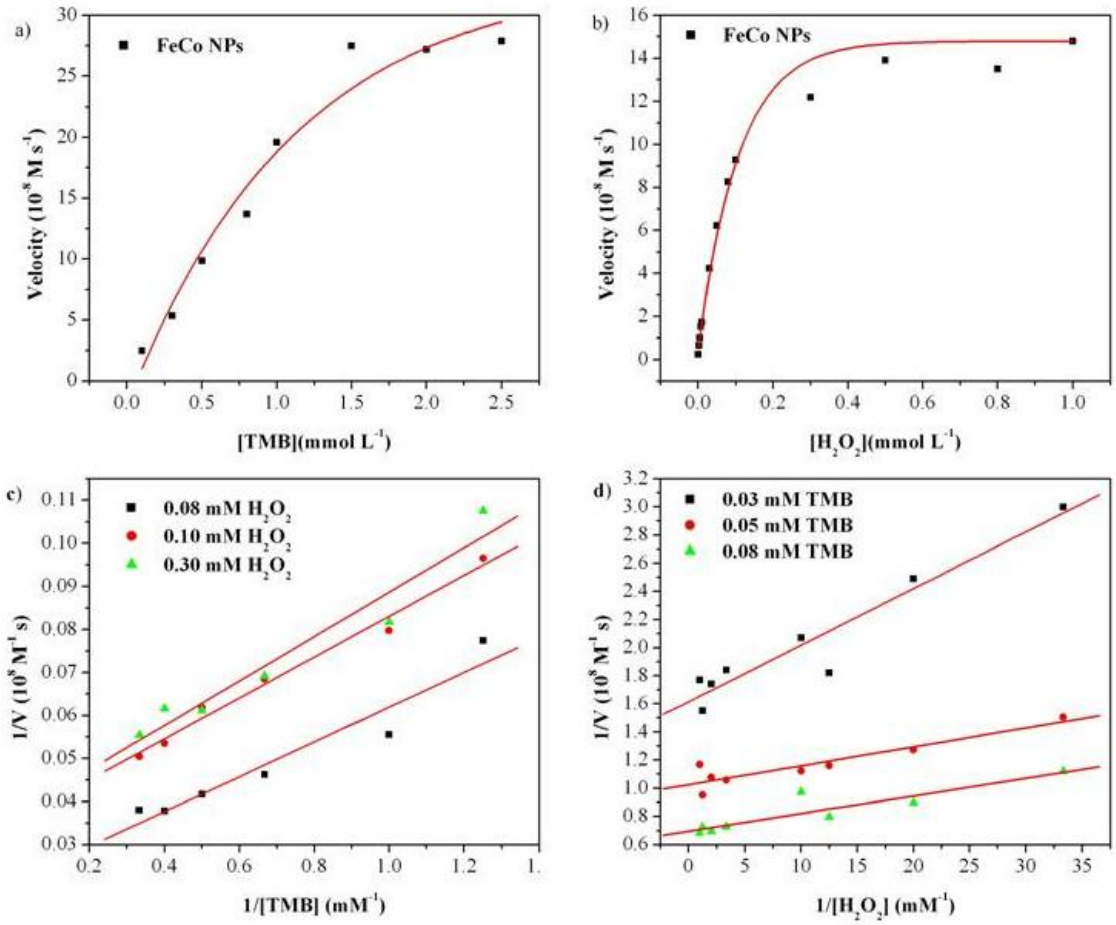

Figure S9. Steady-state kinetic assay and catalytic mechanism of $Fe_{0.5}Co_{0.5}$ NPs (a–d). The velocity (v) of the reaction was measured using 3.5 μg mL^{-1} $Fe_{0.5}Co_{0.5}$ NPs in pH 4.0 acetate buffer at 35 °C (a, b). (a) The concentration of H_2O_2 was 50 mM and the TMB concentration was varied. (b) The concentration of TMB was 0.8 mmol L^{-1} and the H_2O_2 concentration was varied. (c,d) Double reciprocal plots of activity of $Fe_{0.5}Co_{0.5}$ NPs with the concentration of one substrate (H_2O_2 or TMB) fixed and the other varied.

Supplementary Material (ESI) for Chemical Communications
This journal is (c) The Royal Society of Chemistry 2013

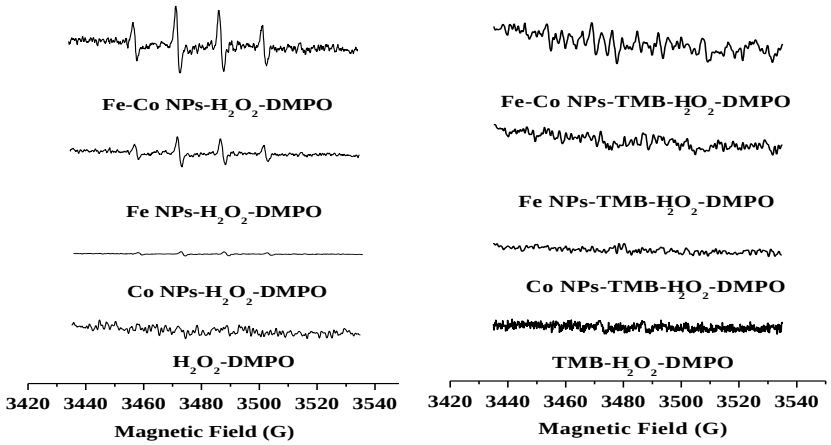

Figure S10. Spin-trapping ESR spectra of $OH^{\bullet}$ radicals in the H_2O_2-DMPO system with and without $Fe_{1-x}Co_x$ NPs (x=0, 0.5, 1) in the absence and presence of TMB. Conditions: 23 mM DMPO, 28 mM H_2O_2, 0.28 mM TMB, 143 mg L^{-1} $Fe_{1-x}Co_x$ NPs (x=0, 0.5, 1), and 0.2 M NaAc buffer.

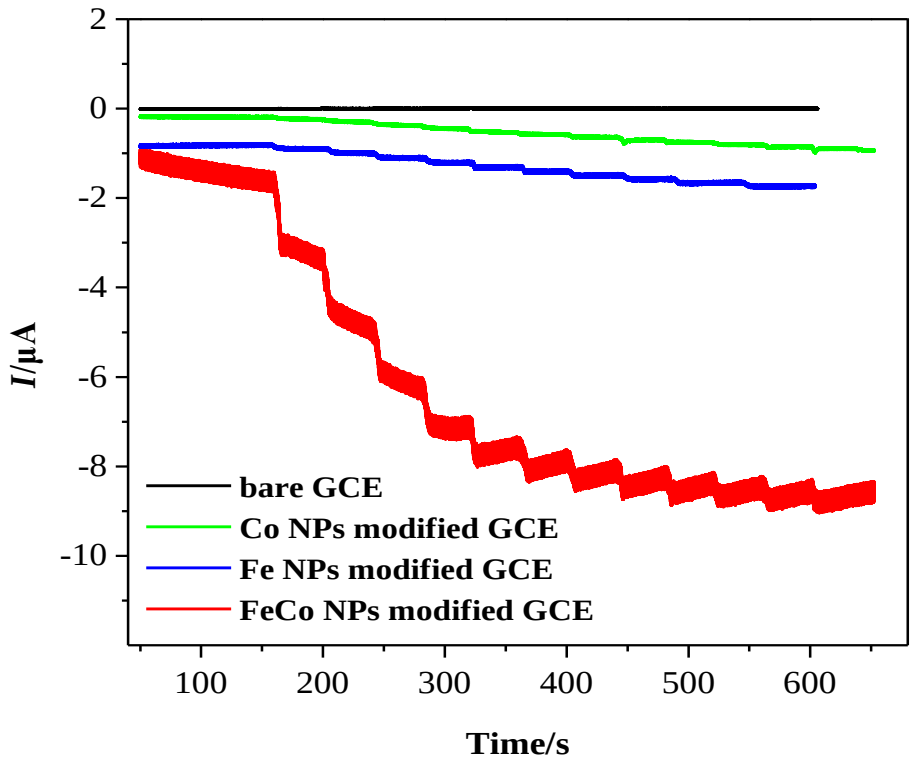

Figure S11. Amperometric response of the modified electrodes to H_2O_2 in a pH 7.0 PBS (0.1 M) at an applied potential of –200 mV upon successive additions of 1.4 mM H_2O_2 with different electrodes at time intervals of 40 s.